Short communication

Discharge characteristic of a non-aqueous electrolyte Li/O$_2$ battery

Sheng S. Zhang*, Donald Foster, Jeffrey Read

U.S. Army Research Laboratory, RDRL-SED-C, Adelphi, MD 20783-1197, USA

ABSTRACT

Discharge characteristic of Li/O$_2$ cells was studied using galvanostatic discharge, polarization, and ac-impedance techniques. Results show that the discharge performance of Li/O$_2$ cells is determined mainly by the carbon air electrode, instead by the Li anode. A consecutive polarization experiment shows that impedance of the air electrode is progressively increased with polarization cycle number since the surfaces of the air electrode are gradually covered by discharge products, which prevents oxygen from diffusing to the reaction sites of carbon. Based on this observation, we proposed an electrolyte-catalyst "two-phase reaction zone" model for the catalytic reduction of oxygen in carbon air electrode. According to this model, the best case for electrolyte-filling is that the air electrode is completely wetted while still remaining sufficient pores for fast diffusion of gaseous oxygen. It is shown that an electrolyte-flooded cell suffers low specific capacity and poor power performance due to slow diffusion of the dissolved oxygen in liquid electrolyte. Therefore, the status of electrolyte-filling plays an essential role in determining the specific capacity and power capability of a Li/O$_2$ cell. In addition, we found that at low discharge currents the Li/O$_2$ cell showed two discharge voltage plateaus. The second voltage plateau is attributed to a continuous discharge of Li$_2$O$_2$ into Li$_2$O, and this discharge shows high polarization due to the electrically isolating property of Li$_2$O$_2$.

Published by Elsevier B.V.

1. Introduction

Non-aqueous electrolyte Li/air battery was first introduced in 1996 by Abraham and Jiang [1], and further developed by many scientists over the world [2–10]. This battery uses a metal lithium anode, a carbon or catalyst-loaded carbon air electrode, and a non-aqueous organic electrolyte, in which the active cathode material is oxygen coming from the environment and the air electrode provides a site for catalytic reduction of oxygen. In organic electrolytes, the catalytic reduction of oxygen is mostly through a two-electron process [1,8], therefore, the overall reaction of a Li/air battery can be written as:

$$2Li + O_2 \rightarrow Li_2O_2 \quad 3.10\,V \quad (1)$$

Depending on discharge current and electrolyte composition, part of the resulting Li$_2$O$_2$ can be further discharged to form Li$_2$O:

$$2Li + Li_2O_2 \rightarrow 2Li_2O \quad 2.72\,V \quad (2)$$

Combining Eqs. (1) and (2) leads to Eq. (3) and a 2.91 V overall voltage:

$$4Li + O_2 \rightarrow 2Li_2O \quad 2.91\,V \quad (3)$$

Therefore, Li$_2$O$_2$ and Li$_2$O coexist in the final discharge products of a Li/air battery [2]. No matter what the final discharge products are, both Eqs. (1) and (3) give a theoretical specific capacity of 3862 mAh g^{-1} vs. metal Li. Due to its high theoretical capacity, the Li/air battery has recently been proposed by U.S. Army as an electrochemical power source for the field charger of Li-ion batteries.

Real capacity of a Li/air battery does not correspond to the theoretical capacity of metal Li due to the insolubility of discharge products (Li$_2$O$_2$ and Li$_2$O) in non-aqueous organic electrolyte. The discharge products are deposited on the surfaces of carbon or catalyst in the air electrode, which blocks oxygen from diffusing to the reaction sites. Therefore, the real capacity that a Li/air battery can achieve is determined by the carbon air electrode, especially by the pore volume available for the deposition of discharge products, instead by the Li anode. In previous works [2,3,5], we have reported the effect of electrolyte formulation and air electrode morphology on the specific capacity of electrolyte-flooded Li/O$_2$ cells in terms of the oxygen solubility and diffusion in liquid electrolyte and the specific surface area and porosity of carbon and air electrode. In this work, we further study the discharge characteristic of Li/air battery and discuss the air electrode model that favors achieving high specific capacity and power capability. To avoid the effects of moisture and carbon dioxide in air, all cells in this work are sealed in a small oxygen bag, and we hereafter call such cells as "Li/O$_2$ cell".

---

* Corresponding author. Tel.: +1 301 394 0981; fax: +1 301 394 0273.
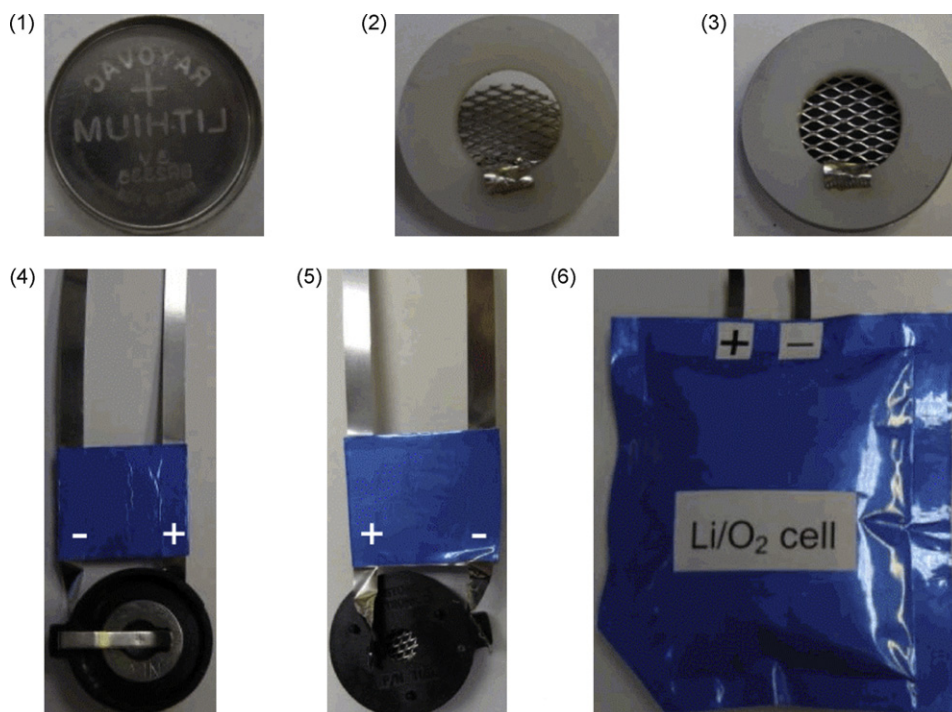*E-mail address:* szhang@arl.army.mil (S.S. Zhang).

Fig. 1. Cell parts for the assembly of Li/air cell and a demonstration Li/O$_2$ cell. (1) Coin cell cap (internal diameter = 22 mm, depth = 3.0 mm) for Li-air cell body and anode current collector, (2) Ni mesh with a silicone rubber disk (diameter = 22 mm, thickness = 3.0 mm, hollow diameter = 7/16 in.) for air cathode current collector, (3) Li-air cell stack, (4) Cell holder and clamper for maintaining constant pressure, (5) Li-air cell, (6) Sealed Li/O$_2$ cell.

2. Experimental

Activated carbon, M-30 (having a specific surface area of 2500–3200 m^2 g^{-1} and a mean diameter of 25–30 μm, Osaka Gas Chemicals Co. Ltd.), was used as the active material of air electrode without the addition of other catalysts. Using polytetrafluoroethylene (PTFE) emulsion (Teflon®, solid content = 61.5%, DuPont Co.) as the binder, two free-standing carbon air electrodes were prepared as the procedure described previously [2,3,5]. One was composed by weight of 92% M-30 and 8% PTFE and the other was composed of 98% M-30 and 2% PTFE. Both electrodes had a thickness range of 0.56–0.63 mm with an M-30 loading of 18.0–19.0 mg cm^{-2} and a porosity of 2.9–3.2 mL g^{-1} (vs. carbon). The porosity of the electrode was calculated from weight change before and after absorption of liquid propylene carbonate, in which a vacuum was applied to ensure a full liquid absorption. The electrode was punched into small disks with an area of 0.97 cm^2, followed by drying at 100 °C under vacuum for at least 8 h for future use. A solution consisting of 0.2 m LiSO$_3$CF$_3$ (Aldrich) dissolved in a 1:3 weight ratio mixture of propylene carbonate (PC, electrolyte grade, Ferro) and 1, 2-dimethoxyethane (DME, electrolyte grade, Ferro) was used as the electrolyte. Fig. 1 shows the parts used for the assembly of Li/O$_2$ cells. The silicone rubber disk that serves as the air-window in part #2 was made by punching a circular hollow equal to the area (0.97 cm^2) of carbon air electrode on a circular rubber disk (diameter = 22 mm, thickness = 3.0 mm). The "punched-out rubber disk" was saved to use as a tool in the next cell assembly.

In a dry-room having a dew point of about −90 °C, a dried Li-air cell (#3 in Fig. 1) was assembled by stacking a Li foil, a Celgard® 3500 membrane, a carbon air electrode and finally part #2 in sequence onto a coin cell cap (part #1). To activate with electrolyte, 200 μL of liquid electrolyte was added through the air-window of cell stack (#3), and then a vacuum was applied to ensure complete wetting. Extra liquid electrolyte was squeezed out by pressing the "punched-out rubber disk" on Ni mesh through the air-window hollow. The electrolyte-activated cell was clamped on a cell holder

(#4) to obtain a Li-air cell (#5), sealing #5 in an O$_2$ bag gives a Li/O$_2$ cell (#6). The same procedure was used for the assembly of a three-electrode Li/O$_2$ cell, except that two pieces of Celgard® 3500 membranes were used as the separator and a small piece of Li foil was sandwiched between two membranes as the reference electrode.

Li/O$_2$ cell was discharged on a Maccor Series 4000 cycler with a 1.5 V cutoff voltage. Before discharge, the cell was rested for 2 h to reach equilibrium between the air electrode and O$_2$ in the bag. After discharge, the cell was dissembled in the dry-room, and the air electrode was washed three times with DME to remove electrolyte salt and dried in air. Microstructure of the washed air electrode was observed using a Nikon Eclipse LV100 microscope equipped with a DXM1200F digital camera. A Solartron SI 1287 electrochemical interface and a SI 1260 impedance/gain-phase analyzer was used for the measurements of polarization and ac-impedance. Polarization test was performed by scanning a discharge current at 0.01 mA s^{-1} between 0 mA and 6 mA. Ac-impedance was potentiostatically measured in a frequency range from 100 kHz to 0.01 Hz with an ac oscillation of 10 mV. All tests were conducted at room temperature (about 22 °C) and there was a 2 h rest between each experiments for these performed on the same Li/O$_2$ cell.

3. Results and discussion

3.1. Theoretical aspects

3.1.1. Li/air battery vs. traditional metal/air batteries

Fig. 2 shows a typical structure of metal/air batteries. The traditional batteries, such as Zn/air battery, use an aqueous alkaline solution as the electrolyte and a catalyst-loaded carbon as the air electrode. In such batteries, oxygen is reduced to form OH$^-$ anions on the surfaces of catalyst and the resulting OH$^-$ anions are subsequently dissolved into electrolyte. Therefore, the air electrode only serves as a reaction site for the catalytic reduction of oxygen. The specific capacities of such batteries are determined either by the
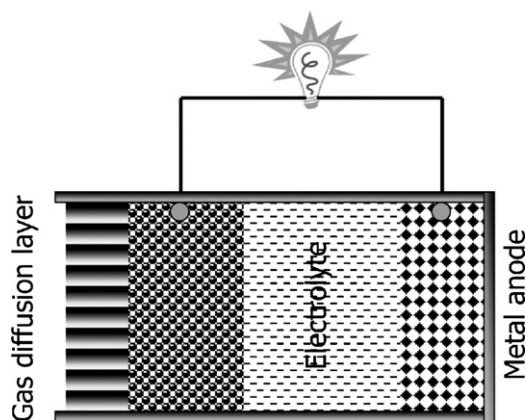
Fig. 2. A typical structure of metal/air batteries, which contains a metal anode, a liquid electrolyte reservoir, an air cathode and a gas diffusion layer to prevent the evaporation of electrolyte solvents.

Fig. 4. Maximum specific capacity of a porous carbon air electrode.

dissolving capacity of the electrolyte or the capacity of the metal anode, and the high power capability is achieved by a "three-phase reaction zone" design of air electrode as shown in Fig. 3a [11,12]. In this model, the air electrode remains partially dry so that air can diffuse in the gas phase throughout the electrode, oxygen is reduced in the gas-catalyst-electrolyte "three-phase reaction zone", and the resulting reduction products of oxygen are immediately dissolved into the electrolyte. The power capability of aqueous electrolyte metal/air batteries is determined by the diffusion and reduction kinetics of oxygen in air electrode.

Li/air battery is different in that it uses an organic electrolyte and the discharge products (Li_2O_2 and Li_2O) are insoluble in the electrolyte. In Li/air battery, the discharge products are deposited on the surfaces of carbon, which prevents oxygen from diffusing to the surfaces of carbon. Therefore, the oxygen reduction cannot remain continuous as indicated in the "three-phase reaction zone" model (Fig. 3a). In this case, we propose a liquid-solid "two-phase reaction zone" for the optimized combination of the specific capacity and power capability (see Fig. 3b). In this model, oxygen reduction occurs on the electrolyte-carbon interface. The air electrode is completely wetted with liquid electrolyte to maximize the reaction area for high specific capacity, and the liquid electrolyte film on the surfaces of carbon remains as thin as possible to minimize the diffusion distance of dissolved oxygen in liquid electrolyte for high power capability. The pores between the wetted carbon particles should not be flooded with liquid electrode so that oxygen can diffuse quickly through the gas phase.

3.1.2. Limitation to the specific capacity of air electrode

Since the specific capacity of the air electrode is determined by the amount of discharge products on the surfaces of carbon, a correlation between the specif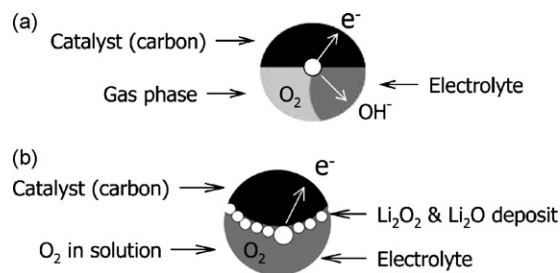ic capacity and electrode porosity is calculated and plotted in Fig. 4, based on Eqs. (1) and (3), and the gravity densities of Li_2O_2 ($2.140\,g\,cm^{-3}$) and Li_2O ($2.013\,g\,cm^{-3}$) crystals. The capacity in Fig. 4 is calculated by assuming all pores are filled with Li_2O_2 and Li_2O, therefore, it can be considered to be the maximum that an air electrode can provide. The normal porosities of carbon air electrodes that were made in this work were between $2.8\,mL\,g^{-1}$ and $3.4\,mL\,g^{-1}$ vs. M-30 carbon. These porosities correspond to a maximum capacity range of 7000–12000 mAh g^{-1} vs. carbon, as indicated by the shadow area in Fig. 4.

Fig. 5 shows the real capacities of four Li/O$_2$ cells at different discharge current densities. First, the specific capacity of carbon is dramatically affected by the discharge current density. Second, the obtained capacities are significantly lower than the maximum expected from Fig. 4. Third, M-30 carbon with very high specific surface area (2500–3200 m^2 g^{-1}) does not lead to high capacity, as compared with Super P carbon that has much lower specific surface area (62 m^2 g^{-1}) while giving higher capacity (2120 mAh g^{-1} in a 1 M LiPF$_6$ PC/DEC electrolyte at 0.05 mA cm^{-2} with a cutoff voltage of 2.0 V) [2]. These results suggest that the specific surface area be not a critical factor for the specific capacity of carbon, and that only few surfaces of the carbon are available for the deposition of discharge products. Based on these facts, an air electrode model is proposed and illustrated in Fig. 6. According to this model, most of the specific surface areas of M-30 are constituted by micro-size pores. These pores are generally filled with liquid electrolyte, into which oxygen is hard to diffuse, not contributing to the specific capacity of the carbon. The similar phenomena have been widely reported for the catalytic reduction of oxygen on a variety of carbons in aqueous alkaline electrolytes [13,14]. The electrolyte-

Fig. 3. Models of the reaction zones for catalytic reduction of oxygen. (a) a "three-phase reaction zone" for aqueous electrolyte metal/air battery and (b) a "two-phase reaction zone" for non-aqueous electrolyte Li/air battery.
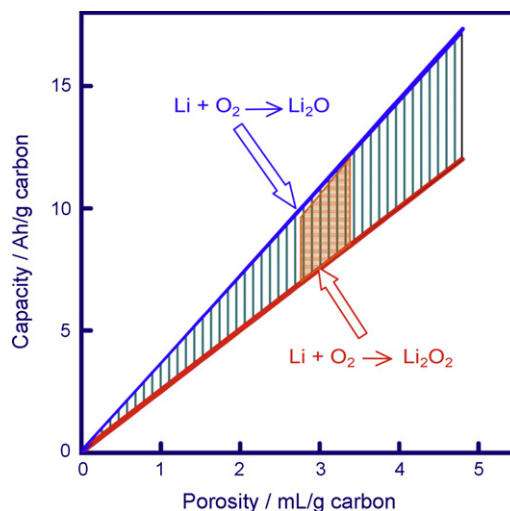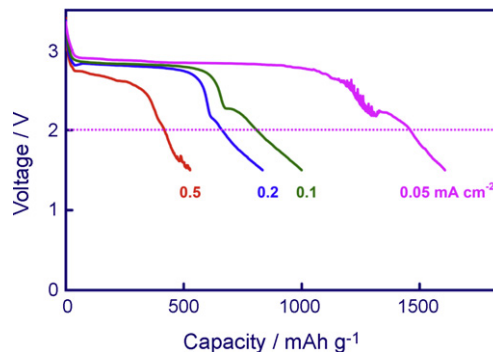

Fig. 5. Discharge curves of four Li/O$_2$ cells at different discharge current densities.
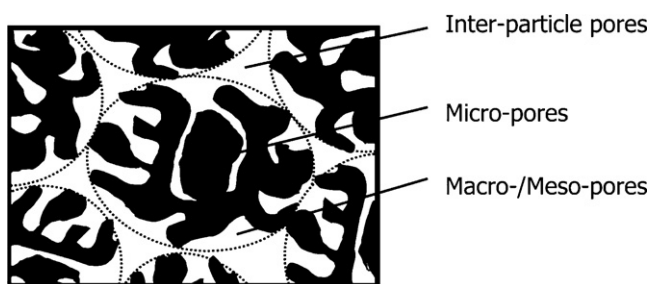
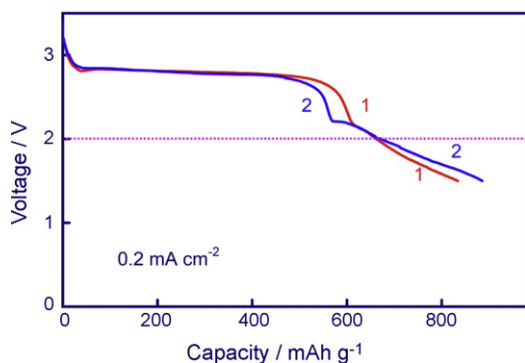**Fig. 6.** A model for carbon air electrode of Li/air battery.

Fig. 7. Discharge curve of Li/O$_2$ cell at 0.2 mA cm^{-2}. (1) 92 M-30/8 PTFE having a porosity of 2.90 mL g^{-1} and (2) 98 M-30/2 PTFE having a porosity of 3.14 mL g^{-1}.

Fig. 8. Potentials of Li anode and air cathode in a Li/O$_2$ cell, which were recorded from a three-electrode Li/O$_2$ cell at a discharge current density of 0.2 mA cm^{-2}.

wetted meso- and macro-size pores are accessible by the dissolved oxygen, however, only few parts of these surfaces show catalytic activity to the reduction of oxygen, contributing to the specific capacity of carbon. The inter-particle pores play a critical role in the power capability of Li/O$_2$ cell. Ideally, these pores should remain open for free diffusion of gaseous oxygen. When these pores are flooded with liquid electrolyte, the Li/O$_2$ cell suffers low specific capacity due to the slow diffusion of the dissolved oxygen in the liquid electrolyte.

3.2. Electrochemical characteristic of Li/O$_2$ cell

3.2.1. Galvanostatic discharge

Fig. 7 shows discharge characteristic of two Li/O$_2$ cells with 92 M-30/8 PTFE (porosity = 2.90 mL g^{-1}) and 98 M-30/2 PTFE (porosity = 3.14 mL g^{-1}) air electrode, respectively. The discharge curves can be divided into the following three voltage regions: (1) rapid decrease in the voltage from open-circuit voltage about 3.4 V to
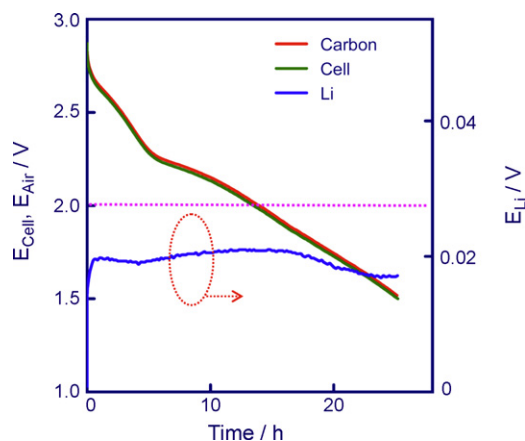
2.8 V, (2) a long discharge voltage plateau at around 2.8 V, (3) a third voltage region that starts at 2.2 V and decreases rapidly. The first voltage region is due to the reduction of oxygen on fresh catalytic sites of carbon, which results in the formation of monolayer coverage (i.e., a nucleation process) of Li$_2$O$_2$. The second voltage plateau is attributed to the reduction of oxygen, during which the particle of Li$_2$O$_2$ grows until the discharge ends (see Eq. (1)). The third voltage region is due to a continuous discharge of Li$_2$O$_2$ into Li$_2$O (see Eq. (2)). Comparing with the theoretical open-circuit voltage (2.72 V, as indicated in Eq. (2)), we find that the third voltage region discharge suffers significant polarization. This is probably because Li$_2$O$_2$ is neither ionically conductive nor electronically conductive, so that the kinetics of Eq. (2) is slow, resulting in high polarization. The third voltage region discharge appears "vanishing" at high discharge currents (see curve at 0.5 mA cm^{-2} in Fig. 5). This is because at high currents, the polarization of Eq. (2) becomes much more significant. In this case the discharge period becomes very short and it cannot be distinguished from the discharge curve of Eq. (1). On the other hand, Fig. 7 shows that two cells have similar capacities (830–890 mAh g^{-1}) despite that the porosity of air electrode in Cell-2 is 0.24 mL g^{-1} higher than that in Cell-1. This result suggests that the porosity contributed by the inter-particle pores, as indicated in Fig. 6, may not be an essential factor for the specific capacity of carbon.

Fig. 8 exhibits potential distributions of the air electrode and Li anode, which were recorded during discharge of a three-electrode Li/O$_2$ cell. It is shown that the potential of the Li anode remains constant at a level of less than 0.02 V vs. Li$^+$/Li, while the air electrode
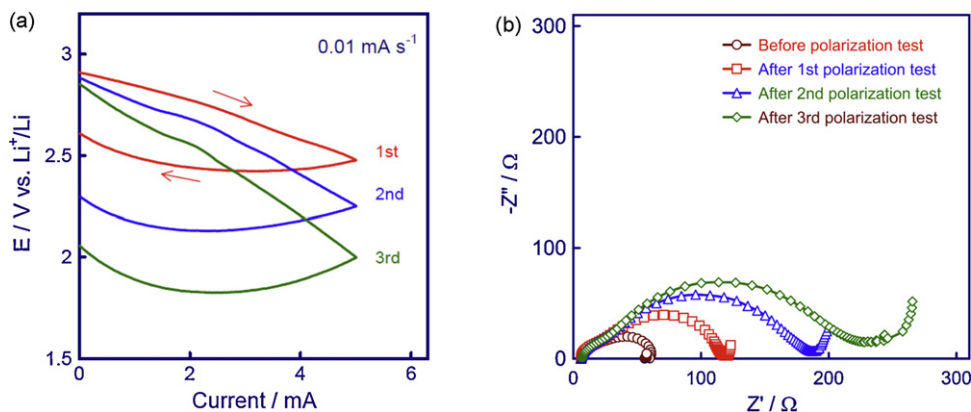

Fig. 9. (a) Three consecutive polarization curves of an air electrode, which were recorded from a three-electrode Li/O$_2$ cell at a current scan rate of 0.01 mA s^{-1} and (b) impedance spectra of the air electrode, measured after each polarization test.
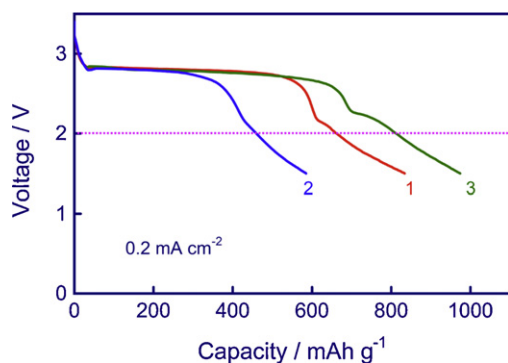
Fig. 10. Discharge curves of three Li/O_2 cells with different electrolyte-filling statuses, which were recorded at 0.2 mA cm^{-2}. (1) With insufficient electrolyte, (2) with excess electrolyte, (3) with appropriate amount of electrolyte.

contributes to most of the overall voltage of the Li/O_2 cell. This result indicates that the power capability of Li/O_2 cells is mainly determined by the carbon air electrode, and that future efforts to improve Li/O_2 cells should be focused on the air electrode.

3.2.2. Polarization analysis

Fig. 9a exhibits three consecutive polarization curves of an air electrode, which were measured from a three-electrode Li/O_2 cell at a current scan rate of 0.01 mA s^{-1}. It is unique that the polarization of the air electrode is increased cycle by cycle. This observation reflects the fact that the discharge products of the Li/O_2 cell are insoluble in the organic electrolyte, they deposit on the surfaces of carbon and prevent oxygen from diffusing to the surfaces of the carbon. The result of polarization experiments also can be explained by impedance data (Fig. 9b), showing that the overall impedance of the air electrode is gradually increased with polarization cycle number. It can be seen from Fig. 9b that the impedance spectrum of the air electrode contains two overlapped semicircles. The semicircle at high frequencies is so small that it is masked by the following large semicircle at low frequencies. Fig. 9b indicates that the change in impedance spectrum mainly occurs in the large semicircle and its following valley at low frequencies. There is little change in the intercept and its following small semicircle at high frequencies. These observations imply that the deposition of the discharge products on the surfaces of carbon not only reduce the kinetics of oxygen reduction, but also affect the diffusion of dissolved oxygen on the electrolyte-catalyst interface.
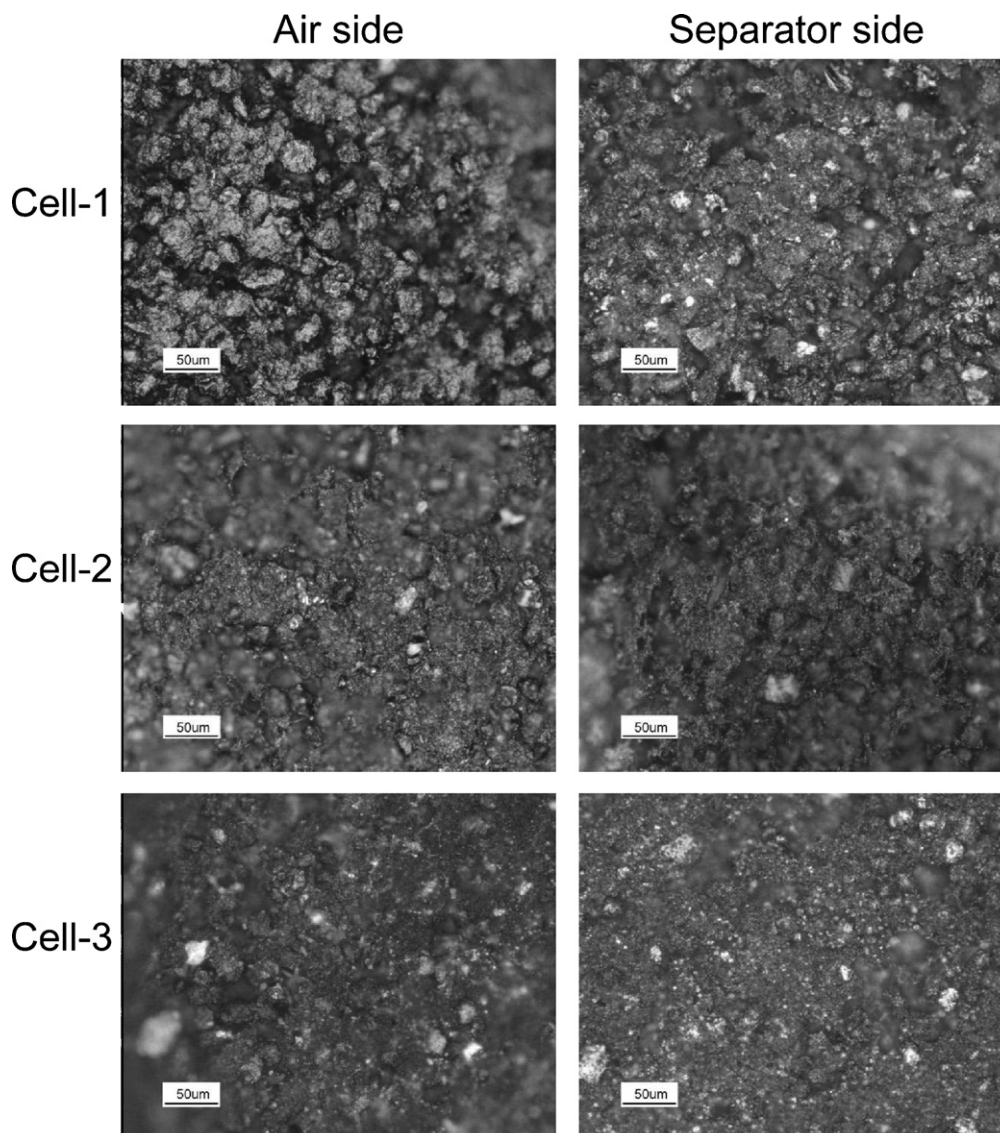

Fig. 11. Microscopic pictures of the carbon air electrodes from three discharged Li/O_2 cells.

3.2.3. Morphology of discharge products

In this work we found that reproducibility for the specific capacity of Li/O$_2$ cells was rather poor in comparison with other Li batteries. The reason turns out to be a variation in the status of electrolyte-filling. Fig. 10 shows discharge curves of three Li/O$_2$ cells with different electrolyte-filling status. To analyze the causes for significant difference in the discharge capacity, we dissembled the cells after discharge and found that Cell-1 contained insufficient electrolyte, Cell-2 had excess electrolyte, and Cell-3 appeared to have appropriate amount of electrolyte. Fig. 11 displays morphologies of the air electrodes from these three cells. It is clear that depending on the status of electrolyte-filling, the discharge products were unevenly deposited onto two sides of the air electrode. As described above, Cell-1 contained insufficient electrolyte, which leaves numbers of inter-particle pores available for the diffusion of gaseous oxygen. Since gaseous oxygen can easily diffuse through the porous air electrode to approach the other side (i.e., separator side), more discharge products are deposited on the separator side (Cell-1, Fig. 11). On contrary, the air electrode in Cell-2 was flooded with electrolyte. In this case gaseous oxygen must dissolve into the electrolyte first, and then diffuse through the liquid electrolyte to the surfaces of carbon. Since the diffusion of dissolved oxygen in liquid electrolyte is very slow, oxygen is hard to reach separator side and its reduction mainly occurs in the air side, as shown by the denser deposition in the air side of Cell-2 (Fig. 11). Cell-3 appeared to have the best status of electrolyte-filling. In this cell, carbon particles were well wetted with the liquid electrolyte while still remaining sufficient pores between the electrolyte-wetted carbon particles for the diffusion of gaseous oxygen. In this case, the discharge products can be evenly deposited throughout the air electrode, resulting in high specific capacity (compare Figs. 10 and 11). The results above reveal that the amount of electrolyte in the cell is essential for obtaining reproducible and reliable capacity data of the Li/O$_2$ cells. A good electrolyte-filling should have the air electrode wetted completely while still remaining sufficient pores for the diffusion of gaseous oxygen.

4. Conclusions

Li/O$_2$ cell is unique in that the discharge products are insoluble in organic liquid electrolyte. This feature requires an electrolyte-catalyst "two-phase reaction zone" model to achieve high specific capacity and good power capability. According to this model, the air electrode should be completely wetted with the liquid electrolyte to supply the maximum reaction area for high specific capacity of carbon. Meanwhile, the air electrode should not be flooded by the liquid electrolyte so that the air electrode has sufficient pores for the fast diffusion of gaseous oxygen to achieve high power capability. The status of electrolyte-filling plays an essential role in the specific capacity and power capability of Li/O$_2$ cells. In addition, the discharge voltage profiles show that two reactions are involved in the discharge process of a Li/O$_2$ cell, i.e., "$2Li + O_2 \rightarrow Li_2O_2$" at 3.10 V and "$2Li + Li_2O_2 \rightarrow 2Li_2O$" at 2.72 V. The latter reaction suffers high polarization due to the electrically isolating property of Li$_2$O$_2$ and its appearance depends on the discharge current and electrolyte composition.

References

[1] K.M. Abraham, Z. Jiang, J. Electrochem. Soc. 143 (1996) 1.
[2] J. Read, J. Electrochem. Soc. 149 (2002) A1190.
[3] J. Read, K. Mutolo, M. Ervin, W. Behl, J. Wolfenstine, A. Driedger, D. Foster, J. Electrochem. Soc. 150 (2003) A1351.
[4] T. Kuboki, T. Okuyama, T. Ohsaki, N. Takami, J. Power Sources 146 (2005) 766.
[5] J. Read, J. Electrochem. Soc. 153 (2006) A96.
[6] A. Dobley, C. Morein, R. Roark, 210th ECS Meeting, Abs. #391, Cancun, Mexico, Oct. 29-Nov. 3, 2006.
[7] S.S. Sandhu, J.P. Fellner, G.W. Bructchen, J. Power Sources 164 (2007) 365.
[8] A. Debart, J. Bao, G. Armstrong, P.G. Bruce, J. Power Sources 174 (2007) 1177.
[9] J.P. Zheng, J. Electrochem. Soc. 155 (2008) A432.
[10] S.D. Beattie, D.M. Manolescu, S.L. Blair, J. Electrochem. Soc. 156 (2009) A44.
[11] C.H. Hamann, A. Hamnett, W. Vielstich, Electrochemistry, Wiley-VCH, Weinheim, 1988, p. 366.
[12] S.W. Eom, C.W. Lee, M.S. Yun, Y.K. Sun, Electrochim. Acta 52 (2006) 1592.
[13] A.J. Appleby, J. Marie, Electrochim. Acta 24 (1979) 195.
[14] D.Y. Qu, Carbon 45 (2007) 1296.